

# Electrochemical microfabrication by laser-enhanced photothermal processes

by R. J. von Gutfeld  
K. G. Sheppard

**Laser-enhanced processes have found an increasingly important role as the interest in microfabrication continues to grow. An especially attractive feature of laser processing in liquids is the ability to obtain maskless patterning in the form of material deposition or dissolution, dictated by the path of the focused laser on the sample. In the present discussion we review theoretical and experimental aspects of laser-enhanced plating and etching for a variety of materials. Some of the substrates readily etched with the help of the laser are extremely difficult to process by conventional methods. Even though the laser processes can handle materials only in a serial manner, the plating and etching rates in certain instances are sufficiently rapid to make them competitive with batch processing methods. This is particularly interesting as it pertains to laser-enhanced jet plating of copper and gold, where rates as high as 50 and 20  $\mu\text{m/s}$  have respectively been obtained.**

©Copyright 1998 by International Business Machines Corporation. Copying in printed form for private use is permitted without payment of royalty provided that (1) each reproduction is done without alteration and (2) the *Journal* reference and IBM copyright notice are included on the first page. The title and abstract, but no other portions, of this paper may be copied or distributed royalty free without further permission by computer-based and other information-service systems. Permission to republish any other portion of this paper must be obtained from the Editor.

## Introduction

Laser processing of materials in liquid media has been of considerable interest for some time. In this paper we review the theory and experimental results of photothermally enhanced laser plating and etching to achieve rapid maskless patterning. In all instances the substrate undergoing processing is immersed in a liquid, generally an electrolyte, and the plating and etching enhancements result from photothermal mechanisms rather than photochemical ones, the latter most often associated with semiconducting materials. The enhanced processes provide both high-speed and highly localized material deposition or removal, making these techniques valuable in the field of microfabrication. The first published data on laser-enhanced plating appeared in 1979 [1]. Subsequently, numerous additional experiments were undertaken that include investigations of laser-enhanced plating of both elemental and alloy metals as well as etching of a wide variety of materials.

In addition to laser-enhanced electroplating and electro-etching, there exist related plating and etching processes that require no external voltage sources, generally classified as *electrodeless*. This category includes

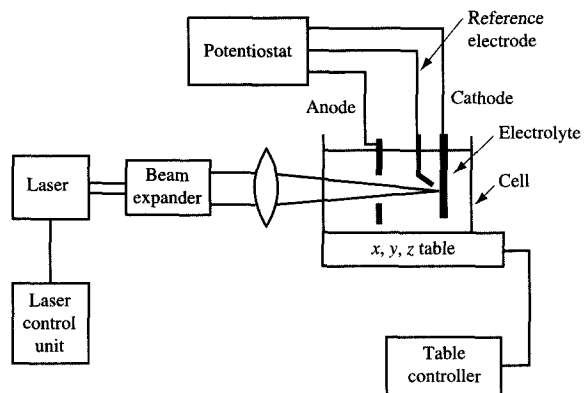


Figure 1

Experimental laser-enhanced plating/etching setup showing the incoming laser, beam expander, focusing lens, and sample cell. A computer is used to move the sample with respect to the laser. A three-electrode system is shown to provide cathode, anode, and reference potential. A video system can be included to image the pattern as it is being formed.

1) electroless, 2) thermally or laser-induced exchange plating (also referred to as the "thermobattery" effect), and 3) laser-enhanced disproportionation. An electroless plating process utilizes an electrolyte containing a reducing agent which provides the electrons required for reduction of the ion to be deposited via multistep chemical reactions. Laser-enhanced exchange plating may occur when a difference in local rest potential exists between two adjacent portions of a substrate due to a temperature gradient. Disproportionation due to local intense heating causes certain solutions to dissociate or decompose, leaving a deposit at the solution/solid interface. Generally, such deposits tend to be porous, with a rough surface morphology, thereby limiting their usefulness for microelectronic applications.

Analogous to the laser-enhanced *electrodeless* plating process is laser-enhanced chemical wet etching, which also occurs without the application of an externally applied voltage. The focused laser produces an increase in the local rate of an oxidation reaction leading to material dissolution. The accompanying simultaneous reduction process typically takes the form of hydrogen evolution. Laser-enhanced electro-etching gives rise to rapid local material removal and is the inverse of laser-enhanced electroplating, with a positive potential applied to the workpiece.

#### • Experimental arrangement

A simple schematic of an experimental laser-enhanced plating/etching setup is shown in **Figure 1**. A focused laser

beam is directed onto the sample contained in a cell via simple optics, here including a beam expander and a high-quality positive lens for beam convergence. To achieve micron-sized patterning, the sample and sample cell are affixed to a computer-driven table. The table allows for relative motion between the laser and sample to provide patterning or "laser writing" capability. In general, sample motion is considerably simpler to achieve than beam steering, although computer-driven mirrors have also been utilized in some experiments [1]. For electroplating and electro-etching, a potentiostat provides the requisite voltages to the sample, a counter and reference electrode. The plating current is then a function of the difference between the reference electrode and the cathode.

#### • General theory

The detailed theory of laser-plating and etching-enhancement mechanisms was first described by Puppe et al. based on experiments using specially patterned cathodes deposited onto glass substrates [2, 3]. A top copper metallization layer deposited onto the glass substrate was completely masked off with photoresist except for a small hole (of the order of 200  $\mu\text{m}$  in diameter). The area defined by the small hole functioned as a microcathode, in contact with a copper sulfate electrolyte. Using a three-electrode configuration, it was possible to monitor the cathode current density as a function of the applied overpotential, both with and without laser radiation incident on the cathode. The overpotential is the difference between the potential to which the electrode is driven and that of the electrode at its equilibrium or rest potential (terms used interchangeably). Electrode potentials are measured relative to that of a reference electrode immersed in the same electrolyte. The rest potential in this system is the one at which copper deposition and dissolution are in balance, resulting in no net current flow across the electrode/electrolyte interface. As the applied potential is made more negative (cathodic) than the rest potential, the electrode (cathode) is driven out of equilibrium, and a net current flows across the interface associated with the deposition of copper ions and their neutralization by externally supplied electrons. Results are shown in **Figure 2**. At the lowest overpotentials (overvoltages), a local increase in temperature due to laser heating at the liquid–cathode interface results in an increase in the charge transfer rate, reflected in an increase in the plating current. The plating-current density  $i$  at these relatively low overpotentials is given by the Butler–Volmer equation [3, 4]

$$i = i_0 \left[ \exp(1 - \beta) \frac{\eta F}{RT} - \exp\left(-\beta \frac{\eta F}{RT}\right) \right],$$

where  $i_0$  represents the exchange current density,  $\beta$  an exchange coefficient,  $\eta$  the overpotential,  $R$  the gas constant, and  $T$  the absolute temperature. The exchange current density is governed by the relation

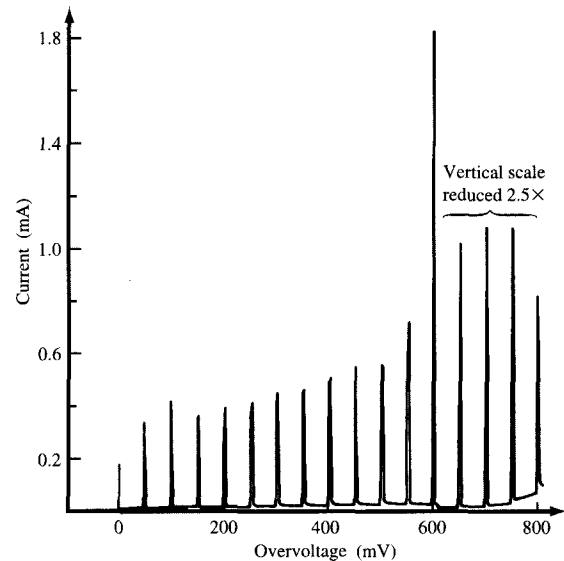
$$i_0 = nF \frac{kT}{h} C_A \exp [(-\Delta G_c + \beta F \Delta \phi_c)/RT],$$

where  $n$  is the valence state of the ion undergoing reduction,  $F$ , Faraday's constant,  $\Delta G_c$ , the chemical free energy of the activation,  $C_A$ , the ion concentration per square centimeter,  $h$ , Planck's constant,  $k$ , is the Boltzmann constant, and  $\Delta \phi_c$ , the equilibrium potential. Since the temperature dependence of  $i_0$  is dominated by the Arrhenius exponential term,  $\exp(-\Delta G/RT)$ , the kinetics of the reaction always increase with increasing temperature, as described earlier [2–4]. Thus, at these low overpotentials, the plating current increase is attributed to an increase in kinetics. A second effect contributing to the enhanced plating rates as determined in the Cu/Cu<sup>2+</sup> system is a positive shift in rest potential with increasing temperature. This shift causes the plating current to be higher for a fixed applied potential, due to laser heating of the cathode/electrolyte interface. In general, this shift is not necessarily in the positive direction and in fact has been observed to be negative for a Ni/NiSO<sub>4</sub> system [3]. At the higher applied overpotentials approaching the mass-transport-limited regime, the large temperature gradients induced by the local laser heating produce substantial microstirring of the electrolyte at the cathode interface. This in turn results in replenishment of the otherwise depleted ions in the diffusion layer. In general, the limiting current density  $i_L$  is given by

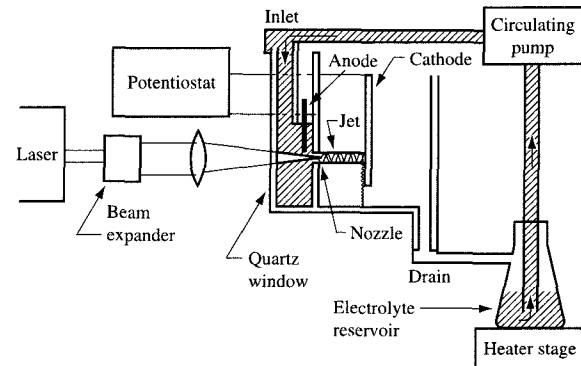
$$i_L = nFDC/\delta.$$

The effect of microstirring decreases the diffusion layer thickness  $\delta$ , thereby increasing the limiting current density, consistent with observation. Here,  $D$  is the ion diffusion constant, and  $C$  the bulk molar concentration of the electrolyte away from the immediate cathode region.

A further increase in the plating rate can be achieved by providing an even faster resupply of ions into the diffusion region than is possible by microstirring. This has been accomplished in the past by the use of a jet of electrolyte, the process referred to as jet plating. For plating processes that are not 100% efficient (that is, where not all of the current is used to achieve reduction of the ion to be deposited—e.g., gold plating from gold cyanide solutions), the combination of a laser with a jet has provided the highest gold plating rates yet achieved [5, 6]. In this configuration, a laser is focused into a pressurized jet stream of electrolyte, shown in **Figure 3**. This system uses only two electrodes operating galvanostatically, that is, with current between the anode



Plating current as a function of overvoltage taken for copper deposition on a microcathode 200  $\mu\text{m}$  in diameter. Note the large enhancement in plating current when the laser is incident on the cathode represented by the sharp spikes in cathode current. From [2], reprinted with permission.



Laser-jet plating system showing the collinear jet and laser beam incident on the cathode. Plating is limited to the region on which the laser jet is incident. From [5], reprinted with permission.

and cathode (substrate undergoing plating) held constant. This mode of operation differs from the aforementioned potentiostatic mode, where the voltage between the reference electrode and the cathode can be set, making

the cathode current the dependent variable [1]. With the focused laser beam directed into the jet, the light becomes trapped, the jet stream acting as a light guide. In this mode, local laser heating, cathode current and a resupply of ions are restricted to a region of the cathode defined essentially by the area of the incident jet. This area also determines the region of deposition. Maskless patterning is again obtained most readily by movement of the sample with respect to the jet stream. As is shown later, laser-jet plating not only enhances plating rates but also improves the morphology of the deposit, as demonstrated for both gold and copper high-speed depositions [6, 7].

- *Theory of alloy plating*

As already noted, laser heating can influence the rest potential and, more profoundly, the kinetics of deposition. In alloy plating, the composition and morphology of the deposit are dependent upon the actual deposition potential (which may be very different from the rest potential), and on the partial kinetics of each depositing ion. In most alloy systems, hydrogen discharge is also typically present as a partial reaction. Laser heating effects on hydrogen discharge kinetics can possibly influence the fraction of the current carried by hydrogen discharge and therefore the efficiency of metal deposition. Furthermore, the codepositing ions may have a mutual effect on alloy electrocrystallization. Thus, deposition of an alloy presents a far more complex environment on which to impose laser enhancement than does deposition of a single metal.

The factors that influence the composition of electrodeposited alloys have been comprehensively described by Brenner [8] and more recently summarized succinctly by Landolt [9]. Brenner has classified alloy systems into various types depending on their behavior. A major distinction exists between "normal" systems, in which the more noble species deposits preferentially, and "anomalous" systems, in which the less noble species is favored. (The term *more noble* refers to a more positive rest potential.) The latter effect can arise from a number of factors, including significant difference in exchange current densities, Tafel slopes (slopes resulting from a plot of the overpotential  $\eta$  versus the natural log of the plating current), and transport limitations for the partial reactions.

Increased temperature due to laser heating can in principle influence composition by a number of means. The deposition potential typically becomes more noble with increasing temperature because of a reduction in overpotential [8]. The extent of this reduction may be different for each of the cathodic partial processes. Polarization, measured by the overpotential, may be due to activation processes or dominated by transport limitations. Activation polarization is due to the steps

needed to take an ion across the double layer, to undergo electron transfer, and, in the case of a metal species, to become incorporated into the solid. Increased temperature can influence the various contributors to activation, e.g., the rate of surface diffusion to growth sites.

In addition to the influence the elevated temperature has on the activation process, elevated temperature also plays a role in increasing the supply of ions to the electrode by both diffusion and convection. Often one or more of the partial processes is transport-limited. Heating can therefore change the relative rate of codeposition of the components and cause a significant change in composition. Commonly, this enhances the deposition of the species that was already preferentially deposited at lower temperature. This is certainly the case with "normal" alloy systems [8]. The result is that at an elevated temperature one may very well find only a single metal component in the deposit from an electrolyte that produced significant alloy codeposition at low temperature.

For example, Khan et al. [10], in evaluating gold-alloy plating electrolytes (Au-Fe, Au-Co, and Au-Ni) as candidates for laser deposition, measured electrodeposit compositions obtained at elevated temperatures in a special high-pressure cell. They found that in Au-Fe the iron content was reduced almost to zero as temperatures went above 70°C. For the Au-Co and Au-Ni there was some initial increase in the cobalt or nickel at lower temperatures; however, this trend reversed, and gold became strongly favored at temperatures above 80°C, with little codeposition of the other element.

It is clear that imposing laser-induced thermal effects on the complex interplay of variables that influence alloy deposition makes prediction of the results almost impossible. It is highly unlikely that one can employ the same formulation for laser alloy plating that is used to obtain a specific alloy by conventional plating. Thus, the electrolyte must be formulated specifically for laser plating and its performance tested in that mode.

## Experimental results

- *Electroplating*

The earliest results on laser-enhanced plating were reported in 1979 using optically transparent insulating substrates of greatly differing thermal conductivity, each overcoated with a thin but *optically opaque* metallic film to make the substrate electrically conducting [1]. A two-electrode anode-cathode system was used, with laser light directed first at the electrolyte-metallized interface. In a second set of experiments, light was directed through the back of the transparent substrate onto the substrate/metallization interface. From these results it was determined that the effect of the laser on the plating

mechanism is principally thermal rather than photochemical in nature, since depositions occurred for both types of illumination. When substrates of high thermal conductivity (sapphire instead of glass) were used, the plated spot dimensions had larger diameters and smaller thicknesses for equal laser-incident power densities, consistent with the higher thermal diffusivity of the substrate and the proposed thermal model. Laser plating of copper, gold, and nickel was obtained in the form of lines and spots. Enhancements (ratios of plating rates with and without the laser) ranged between factors of 100 and 500. Copper lines as narrow as 2  $\mu\text{m}$  in width were deposited on predeposited copper on glass, demonstrating the ability to use laser-enhanced plating for the repair of open microcircuits [2]. This type of repair would require a brief etch after the laser-enhanced deposition to remove the predeposited thin copper layer, which would otherwise cause shorts to the existing lines. Three-dimensional temperature calculations to determine the temperature dependence of laser-enhanced gold plating were undertaken by Kuiken et al. [11]. Experiments to corroborate the thermal model utilized several films of low-thermal-conductivity nickel-phosphorus deposited onto highly thermally conducting cathodes of copper-zinc to determine the plating onset as a function of incident laser power. The thermal barrier layers were found to cause a localized increase in the temperature rise of the argon-laser-irradiated thin-film/cathode structure, even for barrier layer thicknesses as thin as 4  $\mu\text{m}$ . A local substrate temperature rise of as much as a factor of 4 was found compared to that without irradiation, the barrier film acting to limit the lateral spread of absorbed laser energy by confining the energy to a smaller area. The low-conductivity film makes it possible to obtain gold spots using a flux of only 50  $\text{kW/cm}^2$  compared to 250  $\text{kW/cm}^2$  in the absence of the thermal barrier. The data thus help to corroborate the thermal nature of the enhancement mechanism. In addition, the results suggest an important application, that of maskless plating of electrical connectors, limiting the gold deposit to only essential regions of electrical contact. Thus, laser spot plating has the potential for substantial precious metal savings in the connector industry.

Depositions of platinum, gold, and nickel on InP have been demonstrated by Karlicek et al. [12] using an excimer-pumped dye laser at a 10-Hz repetition rate directed onto the substrate. Laser wavelengths ranged from 580 to 720 nm. The InP substrates were submerged in chloroplatinic or chloroauric acids for the platinum and gold depositions, respectively, while nickel sulfate was used for the nickel deposits. No external voltage was applied. Smooth, oriented films up to 0.5  $\mu\text{m}$  in thickness were obtained. Some alloying was observed as the laser caused surface melting of the substrate, an effect which

enhanced the utility of the thin films as ohmic contacts to the semiconductor. A thermal mechanism is considered as the only possible explanation for the results, since similar depositions under similar conditions were obtained on both n- and p-type InP substrates.

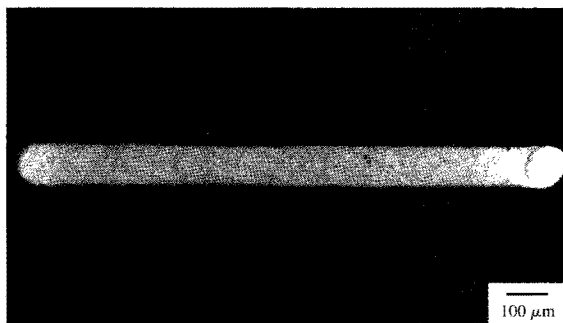
Laser-enhanced zinc deposits have been reported using a pulsed YAG laser [13]. The electrolyte consisted of zinc sulfate with a supporting electrolyte of sodium sulfate. Plating current enhancements (proportional to the plated thickness enhancements) of up to a factor of 5 were observed for depositions using laser irradiation compared to those without the laser at low overpotentials. This enhancement is again attributable in part to a positive shift in the rest potential with increasing temperature resulting from an increase in laser power incident on the cathode. The morphology of the deposits was also greatly improved, as revealed by SEM micrographs which showed a coalescence of islands and a smoothing of a porous dendritic structure due to the increase in diffusion and nucleation rates with increased temperature resulting from laser absorption. The enhanced diffusion may be due in part to melting during the 8-ns laser pulse with estimated peak powers of  $3 \times 10^7 \text{ W/cm}^2$ .

Hsiao and Wan used an argon laser to deposit copper in a manner similar to that described by Pupipe et al. [2] and thermally modeled the process to correlate laser power with plating rates [14]. An estimate of the convective heat loss to the electrolyte at the electrolyte/electrode interface is included in their model. While an extremely high plating rate was obtained (25  $\mu\text{m/s}$  in the mass-transport-limited region), it is clear from micrographs of cross-sectioned deposits that the films are quite porous and therefore not suitable for microelectronic applications. Copper films with excellent surface morphologies, deposited at similarly high rates, have been obtained but required the use of a laser jet to provide the necessary supply of ions to the otherwise depleted diffusion layer, together with localized heat, as described below [7].

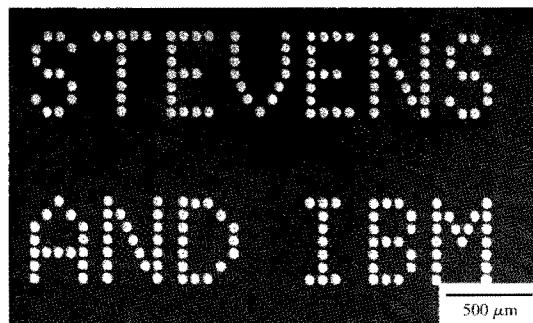
#### • *Laser-enhanced alloy plating*

While in principle it should be possible, there have been only a few studies that have produced alloy codeposition using the laser enhancement method. Friedrich and Raub [15] and Romankiw<sup>1</sup> have obtained minor amounts of codeposition by laser plating from electrolytes similar to those studied by Khan et al. using normal plating at high temperature [10]. These baths are used to deposit hard gold for contacts and contain cobalt or nickel. Both groups obtained no more than a few percent of the alloying element in the deposit. A reason for the lack of success in alloy deposition is that a conventional bath

<sup>1</sup> L. T. Romankiw, unpublished work.



(a)



(b)

(a) Laser-plated line of lead-tin alloy on a nickel film; (b) pattern of dots, approximately  $50 \mu\text{m}$  in diameter, on copper film produced by maskless laser plating. From [17], reprinted with permission.

formulation was typically used. As we have discussed, this likely results in deposition of only one component of the bath. There is a report in the Russian literature of a tin–bismuth nitrate electrolyte that was used to codeposit 2.4 wt% bismuth [16]; the deposits were reported to have good adhesion.

The only study to report significant codeposition of an alloying element by laser plating is for lead–tin from a methane sulfonate electrolyte [17]. An argon ion laser at  $1\text{--}2 \text{ kW/cm}^2$  power density was employed. To counter the tendency in this system to favor tin deposition on heating, the amount of tin in the electrolyte was halved from conventional formulations used for standard electroplating. Polarization measurements were performed, both with and without laser illumination, on copper electrodes covered with photoresist except for small exposed areas the size of the laser beam. The results showed that the laser illumination reduced the deposition overpotential to initiate plating on copper by 20 mV for lead and 30 mV for tin. The reduced values were found to be identical to the overpotentials needed to deposit the individual metals by conventional plating onto themselves (i.e., the copper substrates were preplated with either lead or tin from the same electrolyte). The same effect was obtained with alloy plating. The kinetics for both tin and lead were increased significantly, although not to the extent obtained by Pupipe et al., who used higher laser power densities that resulted in rapid microstirring from incipient boiling [2].

The laser heating appears to have overcome the crystallization overpotential needed to grow these metals on copper. Thus, we have in this system an ability to set the potential at a value less negative than that required to deposit lead, tin, or lead/tin alloys on copper, but more

negative than the laser deposition potentials. In this way it was possible to obtain maskless, localized laser deposition of the individual metals or a range of alloys without significant background plating in the nonilluminated areas. Similar results were obtained on a nickel substrate. Results are shown in Figure 4; the line (a) and dots (b) were obtained with manual translation of the stage holding the substrates.

A problem with the laser-plated lead–tin alloy was an increase of tin content with thickness due to the rising temperature as the laser dwell time increased. Some preliminary data suggest that modulating the laser could reduce this effect.

#### • *Laser-enhanced exchange plating*

Experiments of Kulynych et al. [18] and Pupipe et al. [2] showed that when a copper surface is submerged in a copper sulfate solution and irradiated by a focused laser, local copper depositions occur because of a temperature gradient produced by the absorbed laser radiation (although in general any form of local heating can be used). As described earlier, copper experiences a positive shift in rest potential in the heated region, becoming more cathodic than its cooler periphery. Simultaneous oxidation and reduction occur, but in spatially separated regions of the substrate; the more-cathodic portion of the electrode undergoes copper deposition (reduction); the neighboring less-cathodic region, copper dissolution (oxidation). All of the ions for the deposition process are supplied by the electrolyte, while an equal number are returned to the solution via dissolution of the cooler portion of the substrate. Thus, overall charge conservation is maintained, with no net change in the total or global ion population of the electrolyte. In a related experiment, it has been shown

that when a thin copper film deposited on a glass substrate is subjected to focused laser radiation while submerged in copper sulfate solution, the heated region continues to grow in thickness until electrical contact is broken around its periphery. The loss of contact, and hence the cessation of plating, occurs because of the etching surrounding the heated region [3].

For those electrolyte/metal systems possessing a negative shift in rest potential with increasing temperature, dissolution occurs in the heated region, with simultaneous peripheral plating. This effect has been observed for nickel submerged in a nickel sulfate electrolyte [3].

More recent results on thermally enhanced exchange plating of copper as a function of incident laser power have been performed by Hsiao et al., again using copper sulfate solution and a copper electrode in a thermogalvanic cell [19]. A focused argon ion laser was used to produce the localized heating. While attributing the local plating at low laser powers to a shift to a more positive rest potential, it was found that at higher laser powers simultaneous plating and etching can occur in the *heated* region because of overheating, resulting in a secondary chemical reaction. At these high power levels, the deposits are extremely porous. Exchange plating has also been used to fabricate or "write" copper lines of the order of 2  $\mu\text{m}$  in width on lithium niobate substrates onto which an initial copper coating has been deposited [20]. Here, argon laser power levels were in the range of 20 mW.

It is worth noting that exchange plating can also occur when current is passed through a circuit (submerged in copper sulfate solution) having a nonuniform electrical resistivity as a function of its length. Here, joule heating (resistive heating due to current flow) rather than laser heating produces a thermal gradient which results in a buildup of the thinner, more resistive portion of the circuit at the expense of the thicker, cooler portion. This technique has been demonstrated successfully for the repair of damaged (thinned or notched) but still electrically continuous computer board circuits [21].

Disproportionation of certain organometallic solutions has resulted in depositions of Mo and Cr on glass substrates, these substrates forming the sidewalls of a liquid cell container [22]. Several tens of mW of argon laser light were focused onto the glass/solution interface of the solution cell containing  $\text{Mo}(\text{C}_6\text{H}_5)_2$  and  $\text{Cr}(\text{C}_6\text{H}_5)_2$ . Substantial local heating was expected in the focal region, since these solutions are strongly absorbing at wavelengths shorter than 800 nm. Resulting deposits consisted typically of 10- $\mu\text{m}$ -diameter spots. A time delay of several seconds elapsed before the onset of any deposit, consistent with a disproportionation model (referred to as pyrolytic by the authors). Delay time increased with decreasing laser

power, while requisite threshold power increased with solution concentration. Auger analysis of the deposits indicated as much as 10% incorporated carbon, possibly due to decomposition of the benzene at high operating temperatures. The micrographs of the depositions exhibit a porous structure and rough surface morphology. This type of structure was also observed in experiments in which gold was unexpectedly found deposited on the interface of a glass/commercial gold plating solution resulting from intense laser radiation focused in that region, attributable to disproportionation.<sup>2</sup> This same mechanism is also considered to have contributed to gold deposition on p-InP in a sodium gold sulfite plating bath under illumination by a cw argon ion laser [23]. About 4  $\text{kW/cm}^2$  power density was required, resulting in good-quality adherent deposits.

Insulating thin-film patterns have been deposited onto several metal and metallized insulating samples by directing focused argon laser light onto substrates submerged in 0.2-M nickel sulfate solutions with a pH close to neutral (6.5). Typical incident power densities were of the order of  $10^6 \text{ W/cm}^2$ . Film thicknesses as small as 50 nm were obtained with a single scan of the laser beam across the submerged sample. The mechanism for these depositions is explained in terms of local boiling of the electrolyte in the immediate region of the focused laser, leaving a residue in the form of a highly insulating thin film containing constituents of the solute, the presence of the constituents verified by Auger spectroscopic examination [24].

#### ● *Laser-jet plating*

Laser-jet plating has been studied most extensively using a gold cyanide solution for the deposition of soft gold, principally on Be-Cu substrates typical of those used in much of the connector industry [5, 6]. Plating rates as high as  $\sim 20 \mu\text{m/s}$  were obtained using nozzle diameters of the order of 0.3 mm, while rates of  $10-12 \mu\text{m/s}$  resulted from use of a 0.5-mm-diameter nozzle with the same total laser power ( $\sim 20-25 \text{ W}$ , but proportionately decreased laser power density). Detailed studies of surface morphologies as a function of laser power and plating current were undertaken, as described in [6]. Experimental data of plating rates versus incident laser power for a 0.5-mm-diameter nozzle are shown in Figure 5 using a high-gold-concentration solution which is commercially available (4 Tr oz per gallon, Autronex 55 GV). In this higher range of laser power (i.e., power densities greater than  $\sim 1 \times 10^4 \text{ W/cm}^2$ ), the plating rate is approximately linear with power density [6]. However, only very approximate estimates have been made to determine the substrate temperature due to heating by the incident laser power with

<sup>2</sup> R. J. von Gutfeld and L. T. Romankiw, unpublished work.

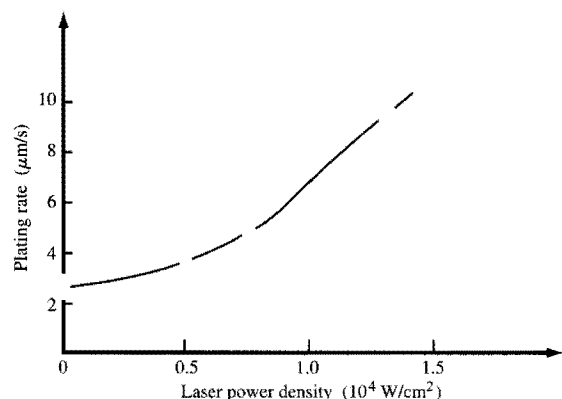


**Figure 5**

Laser-jet gold plating rates as a function of incident laser power for a fixed current density of  $12.5 \text{ A/cm}^2$  using a 0.5-mm-diameter nozzle. From [6], reprinted with permission.

simultaneous cooling from the incident jet stream, the latter generally maintained at  $60^\circ\text{C}$ , the manufacturer's recommended bath temperature.

Deposition with simultaneous cathode current measurements indicates that the higher laser power levels increase the gold plating efficiency; that is, the cathode current utilized for reduction of the gold ion increases from approximately 20% to 60%. The increase in efficiency can be understood in terms of the laser heating, with the resulting local higher temperature favoring the gold deposition reduction process over that of the competing process, the reduction of  $\text{H}^+$  to  $\text{H}^0$ . However, the laser plays an additional important role, that of greatly improving the morphology of the deposit. For example, for gold plating rates of  $2 \mu\text{m/s}$ , using the jet without the laser results in a deposit that is replete with cracks and voids, totally unacceptable for any electronic application. However, under laser-jet plating conditions, even at deposition rates of  $10 \mu\text{m/s}$ , the film morphology, based on examination of cross-sectioned samples, is found to be compact, pore- and void-free. The contrast in film quality is shown in the cross sections of deposits made with the laser jet [Figure 6(a)–(c)] and the jet without the laser [Figure 6(d)–(f)] [4–6].

Laser-jet plating has also been applied to high-speed copper plating [25]. Here there is only one reduction process, so that the plating is generally considered to be 100% efficient. Experimentally, the plating rate was found to be independent of incident laser power, consistent with a 100% efficient plating process (Figure 7). While it is evident that the laser has no effect on the laser-jet plating rate based on measurements of the spot height as a

function of dwell time (compared to the jet-plated spots, no laser), it is found that at the higher plating rates, the resulting deposit morphology is extremely poor for deposits produced without simultaneous laser irradiation. It is believed that the laser promotes higher rates of nucleation and surface mobilities of the deposited atoms. Thus, for laser-jet plating of copper, the resulting morphology was found to be uniform and void-free even for plating rates as high as  $50 \mu\text{m/s}$ , as determined experimentally using a 0.2-mm-diameter nozzle. The effect of the laser on the film surface morphology is shown in Figure 8 for jet-plated spots made with and without laser radiation. The superior structure of the laser-jet-plated spots is quite evident. Similar beneficial effects of the combined use of the laser with the jet were found for cross-sectioned samples of copper.

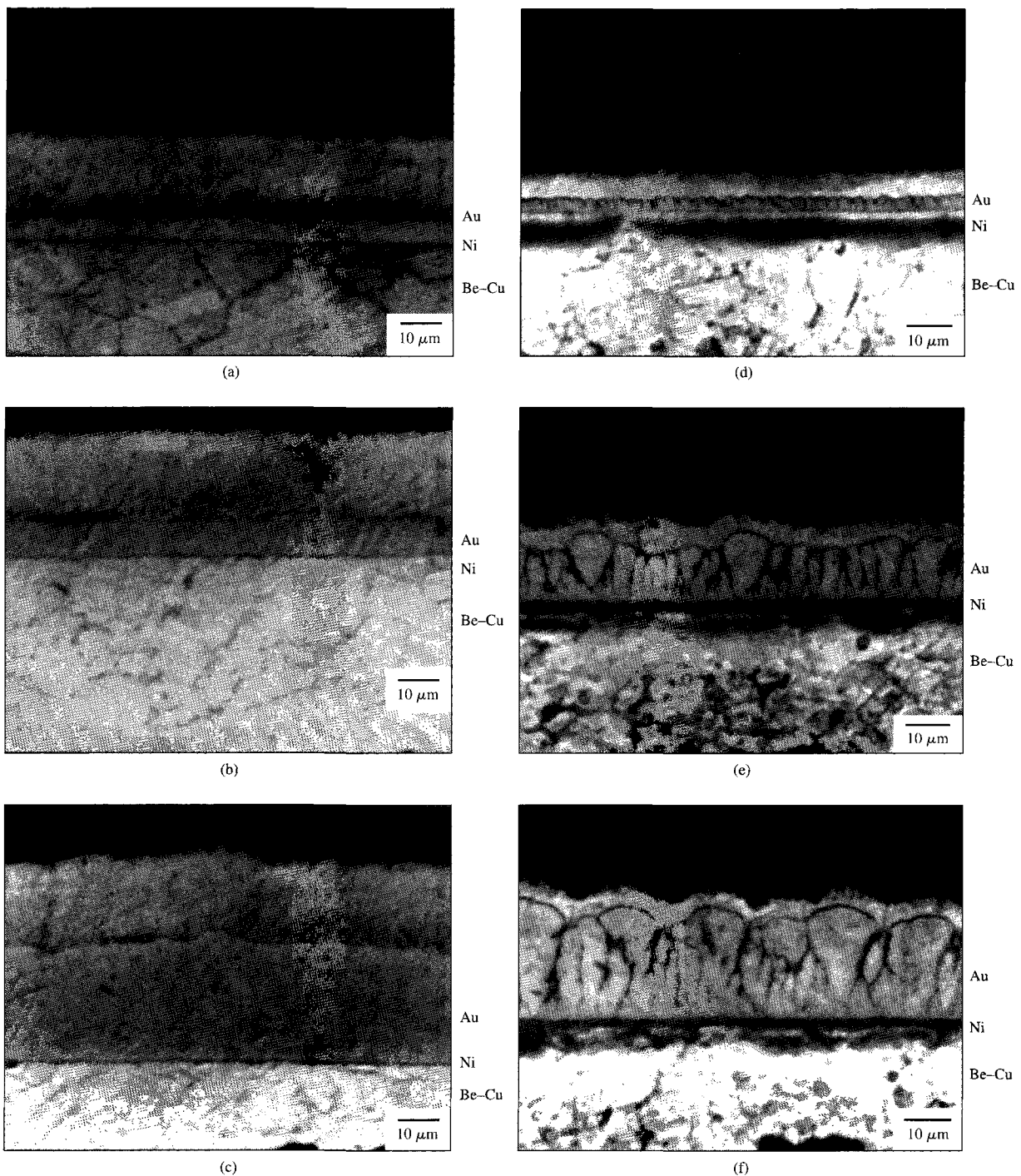
#### • Electroless plating

The most extensive reported results on laser-enhanced electroless plating are described in a U.S. patent by Blum et al. in which nickel was patterned onto glass substrates, the glass predeposited with  $100 \text{ \AA}$  of nickel by vapor deposition [26]. The electroless solution was formulated from nickel sulfate and sodium hypophosphite. The predeposition of nickel makes it possible for the plating to occur without the need for a preactivation step. Argon laser light was focused onto the sample through the solution to approximately a  $150\text{-}\mu\text{m}$  diameter, equivalent to  $1 \times 10^3 \text{ W/cm}^2$  incident on the sample, with a resulting nickel plating rate as high as  $800 \text{ \AA/s}$ . Under similar conditions, background plating rates of only  $0.1 \text{ \AA/s}$  were measured. To ascertain that the enhancement mechanism is not a photo-effect, depositions were also obtained with illumination through the glass, i.e., back-illumination to eliminate the possibility of photons reaching the solution/metallized substrate interface. A compilation of nickel spot deposits made under varying conditions is shown in Table 1.

#### • Etching

Laser-enhanced electro-etching was first demonstrated for fabricating small holes in  $50\text{-}\mu\text{m}$  stainless steel shim stock for the purpose of producing ink-jet nozzles  $50 \mu\text{m}$  in diameter [2]. Here  $\text{NiCl}_2$  was used as the electrolyte. The resulting etched sidewalls were extremely smooth, and the holes required no postprocessing in order to function as nozzles with good droplet formation (Figure 9).

Laser-enhanced chemical etching at high laser power densities has been demonstrated on a number of ceramic materials, principally alumina/TiC, as well as single-crystal silicon, with up to  $20 \text{ W}$  of incident argon ion laser power [27]. These materials were immersed in concentrated KOH solutions through which the laser was focused. Because of the high optical absorption of the materials,



Laser-jet-plated cross-sectioned deposits of gold (a)–(c) deposited on nickel-plated Be–Cu samples 200  $\mu\text{m}$  thick; plating current, 11  $\text{A}/\text{cm}^2$ . The top surface is an overcoat of nickel used to protect the gold during cross-sectioning. Plating times and resulting thicknesses: (a) 0.5 s, 4.5  $\mu\text{m}$ ; (b) 1 s, 8  $\mu\text{m}$ ; (c) 5 s, 30  $\mu\text{m}$ . Deposits made without the laser irradiation are shown in (d)–(f), indicating a structure replete with voids; plating rates approximately 1/3 of those achieved with the laser jet: (d) 1 s, 3  $\mu\text{m}$ ; (e) 5 s, 12  $\mu\text{m}$ ; (f) 10 s, 25  $\mu\text{m}$ . From [4], reprinted with permission.

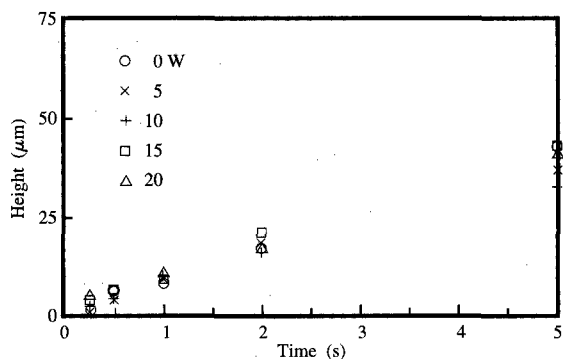


Figure 7

Experimentally obtained copper jet plating obtained with laser power as a parameter (power indicated by symbols on the figure) as a function of time using a 0.5-mm-diameter jet nozzle and 70 mA of plating current ( $\sim 36 \text{ A/cm}^2$ ). From the data, the plating rate is seen to be independent of laser power, but the morphology is greatly improved with the laser jet, as shown in Figure 8. From [7], reprinted with permission.

local temperatures as high as or even above the melt temperature were reached at the electrolyte–substrate interface, resulting in active stirring by the superheated solution. The agitated solution rapidly removes the dissolved material while replenishing the depleted ions of the etching electrolyte. Micron-sized grooves and holes, both vias and through-holes, were obtained. KOH is a known strong etchant for atoms in the  $\langle 100 \rangle$  plane of Si, but a very poor etchant for atoms in the  $\langle 111 \rangle$  plane of Si. However, rapid etching of the  $\langle 111 \rangle$  Si atoms was attained, a result interpreted in terms of the occurrence of local melting and the resulting disruption of the crystal symmetry allowing for etching in other than the original  $\langle 111 \rangle$  orientation. Figure 10 shows data of Si and alumina/TiC etching rates as a function of laser power, while Figure 11 is an electron micrograph of a laser-etched groove in alumina/TiC (using KOH) exhibiting very smooth and regular sidewalls.

Laser etching of vias, blind vias, and grooves in polyimide has also been reported using a focused low-power ( $\sim 100 \text{ mW}$ ) cw argon ion laser incident on the substrate immersed in NaOH solutions of varying concentrations [28]. While ceramics and Si utilized KOH, this etchant is not suitable for use here, since it leads to spontaneous dissolution of polyimide. With NaOH solutions, however, Kapton\*\* volume removal was well controlled, with etch rates as high as  $10^4 \text{ }\mu\text{m}^3/\text{s}$ , resulting in holes with extremely smooth sidewalls. There was no observed etching in regions in which the laser was absent. The fastest etch rates that maintained smooth wall

morphologies were found for NaOH concentrations in the range 5–18 N with linear etch rates up to  $1 \text{ }\mu\text{m/s}$ . However, mixtures of KOH in ethanol/water resulted in even faster rates, of the order of  $3 \text{ }\mu\text{m/s}$ . In general, laser heating of the polyimide speeds the reaction with the etchant, forming soluble compounds which are readily dissolved.

The same laser-assisted technique was also used to etch via holes in Kapton laminated to copper, an important material for interconnection applications on electronic circuit boards. The copper and Kapton were each  $15 \text{ }\mu\text{m}$  in thickness; etching to bare copper was achieved in 20 seconds.

Laser chemical etching experiments using noncorrosive neutral salt solutions have been undertaken by Datta et al. [29]. Etching solutions include sodium nitrate, sodium chloride, and potassium sulfate for laser etching of steel and stainless steel; data are shown for various parameters in Table 2. Etching patterns consisted of arrays of holes as a function of solution concentration, laser power density, and laser dwell time. A maximum etch rate of  $4 \text{ }\mu\text{m/s}$  was obtained with an 0.5-M sodium nitrate solution, as shown in Table 2. The stepwise mechanisms believed responsible for etching involve the formation of a passivating layer which becomes anodic and dissolves because of the enhanced temperature produced by absorption of the laser. The nonirradiated surface becomes cathodic, resulting in hydrogen and/or oxygen evolution. During etching, two processes compete in the region of etching, that of metal dissolution, neutral metal to metal ion (oxidation) and repassivation. The repassivation process is dependent on the particular ions in solution. These experiments demonstrated the feasibility of rapid high-quality etching without the use of environmentally hazardous acid or alkaline corrosive solutions.

Subsequent to the above referenced experiments, laser etching of Cu, Mo, Ni, Nb, and stainless steel immersed in 0.5-M sodium nitrate solution was studied in some detail [30]. Etching results were obtained as a function of laser intensity and laser dwell time. Etch rates up to  $4 \text{ }\mu\text{m}$  were obtained using  $\sim 15 \text{ W}$  of focused cw-argon laser light. Again, etching occurred at or near melting temperatures in reasonably close agreement with calculated values using a three-dimensional heat-flow model for an incident Gaussian beam. The etching process is believed to involve passivation of the surface followed by depassivation via dissolution at the elevated temperatures. A scanning electron micrograph of etched copper after 30 seconds using 10 W of incident focused laser power is shown in the scanning micrograph, Figure 12.

An interesting type of electrodeless laser etching has been described in a patent by Gupta et al. [31]. In their preferred embodiment, a pulsed copper vapor laser (operating at repetition rates of 5–10 kHz, pulse widths

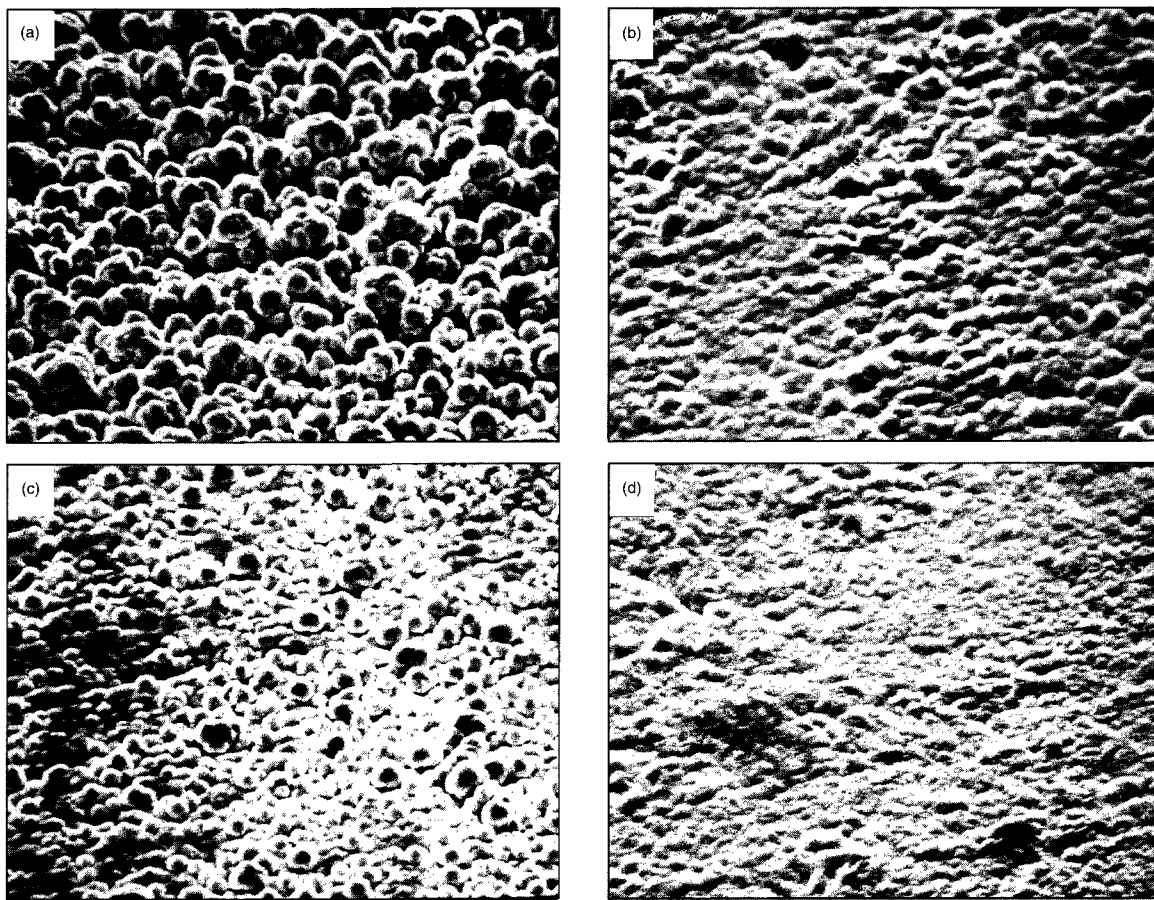


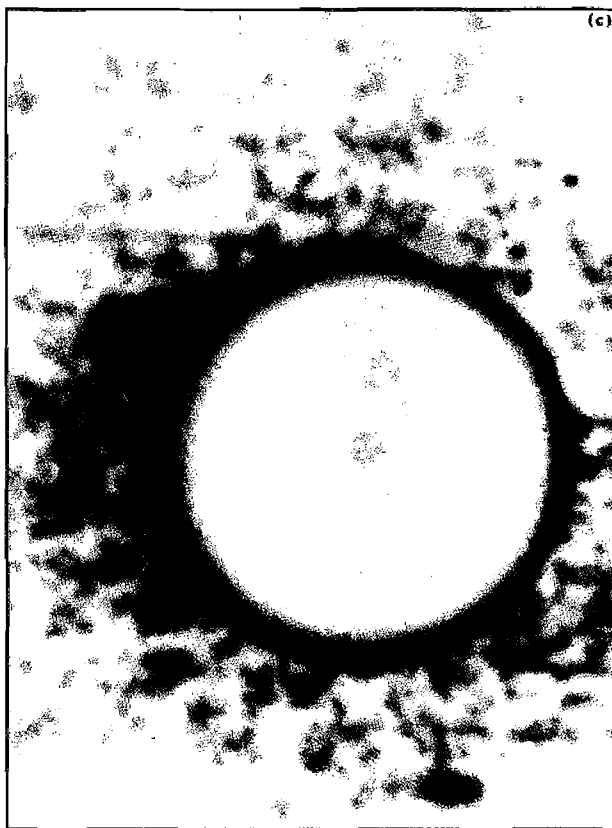
Figure 8

Scanning electron micrographs of the surface morphology of jet-plated (a) and (c) and laser-jet-plated (b) and (d) copper lines at two current densities,  $38 \text{ A/cm}^2$ , (a) and (b) and  $25 \text{ A/cm}^2$ , (c) and (d). A 0.5-mm nozzle diameter and scan speed of  $500 \mu\text{m/s}$  were used. The substrate was Be-Cu and the approximate incident laser power density,  $2 \times 10^3 \text{ W/cm}^2$ . From [7], reprinted with permission.

20–30 ns, with wavelengths a combination of 511 and 578 nm) is one of the light sources used while a focused pulsed YAG or modulated cw argon laser could also be employed. The preferred medium in which the substrate is submerged during etching is water or any nonreacting organic or inorganic liquid. The etching mechanism is believed to be abrupt heating of the substrate followed by strong cavitation (that is, bubble formation and collapse), a phenomenon well known to cause wear on surfaces. The etching process is enhanced by the sudden rise in temperature of the material in combination with the cavitation. With this technique, the authors were able to etch very small as well as delicate parts such as thin-film magnetic heads made of hard ceramic material,

**Table 1** Laser electroless nickel plating [26].

Time (s)	Thickness (Å)	Average diameter ( $\mu\text{m}$ )	Average plating rate ( $\text{\AA/s}$ )
5	2500	$\sim 160$	500
	2100		420
	7400		480
	8000		800
10	7500	175	750
	7000		700
	12000		800
	10000		670
15	9000	170	600
	11000		730



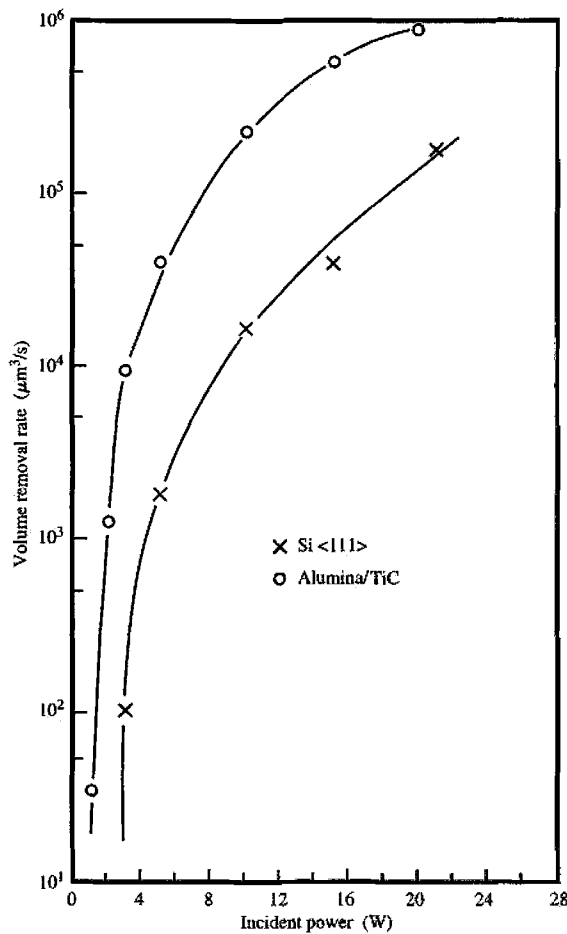
Etched hole in 50- $\mu\text{m}$ -thick stainless steel to form an ink-jet nozzle. From [3], reprinted with permission.

alumina/TiC. At the same time, with the use of noncorrosive liquids, any premetallization not in the region of the laser remains unaffected. In contrast, typical etchants such as KOH or various acids tend to aggressively attack metals as well as the substrate to be etched, making this local cavitation technique very useful for maskless etching of parts containing circuitry.

Additional experiments by some of these same authors showed the importance of bubble formation as well as cavitation in the etching of Mn-Zn ferrite substrates [32]. Both water and KOH were used as the liquid medium in which the substrates were immersed, with the substrates irradiated by either an argon laser pulsed by way of an acoustic modulator or a high-repetition-rate copper vapor laser. With the copper vapor laser, it was found that etching is equally effective in water and in KOH. However, at lower laser repetition rates and longer pulse widths, KOH enhances the laser light reaching the work piece by preventing the bubble that forms during etching from adhering to the substrate. The diameter of bubbles

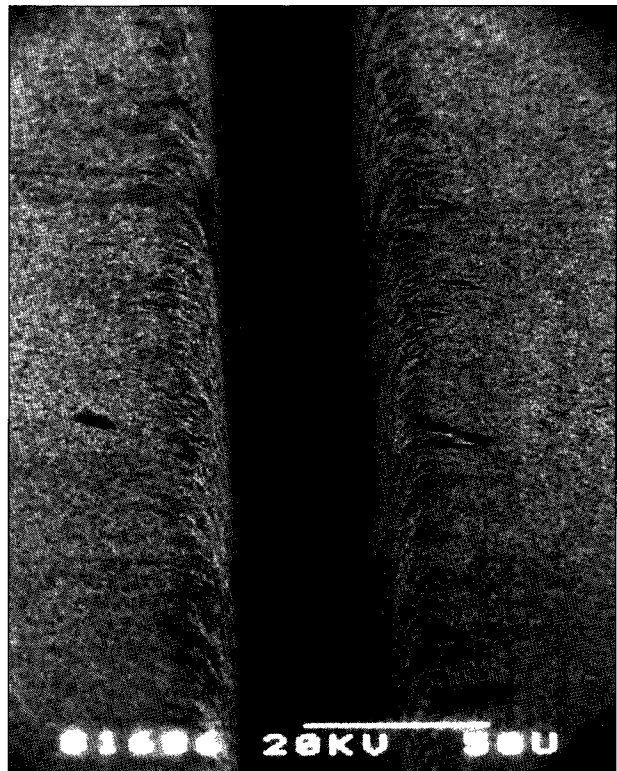
generated at the liquid-substrate interface was measured as a function of laser repetition rate and correlated with the resulting etch rate. A decrease in bubble diameter with increased repetition rate and decreased pulse width was observed. Smaller bubble size and a reduced time during which the bubble adheres to the workpiece results in decreased light scattering and in turn, more rapid etching. The proposed model for etching based on these data includes a combination of melting, fluid stirring, and cavitation. For those cases where the bubbles are very small, cavitation is the main mechanism.

Laser-assisted chemical etching has been investigated in some detail by Nowak et al. on Co, Cr, Cu, and Ti using a focused argon laser of modest laser power (typically of the order of several hundred mW, up to 800 mW) and power

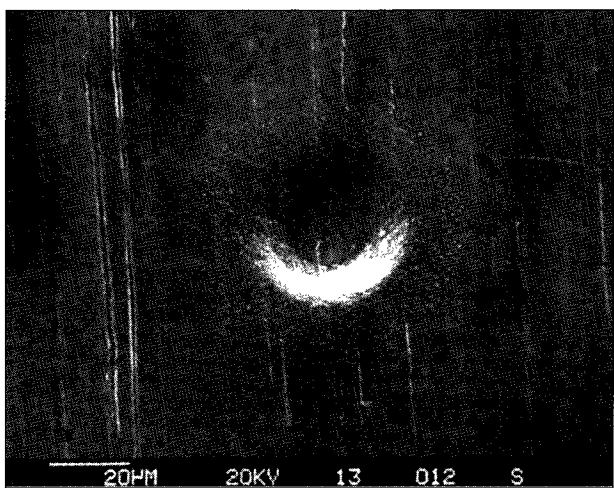


Volume-removal rates as a function of laser power for alumina/TiC ceramic and <111> silicon using KOH as the etchant. From [27], reprinted with permission.

densities well below that required for melting of the sample material [33]. Both holes and lines were etched. Aqueous solutions of phosphoric acid and potassium hydroxide of varying concentrations were used. For cobalt, the ratios of etch rates for laser-illuminated versus dark regions are as high as  $10^6$ . In KOH the etch rates of copper (samples of the order of 1000–5000 Å thick), and Ti thin films (thicknesses of the order of 1000 Å), as well as Co foils, were found to be exponentially dependent on laser power, indicating a thermally enhanced process. For Ti films, an etch rate up to 20 times faster was observed using phosphoric acid. Static etch rates as high as 10  $\mu\text{m/s}$  were observed. Here the basic mechanism is thought to involve an increase in the temperature-assisted dissolution (Arrhenius-type process). Etching was carried out both on films predeposited on glass and on 25- $\mu\text{m}$ -thick foils, the latter fabricated into miniature Ti parts. The laser etching utilized phosphoric acid solutions.



Scanning electron micrograph of groove in alumina/TiC using  $\sim 1.5$  W of focused argon laser power scanned at approximately 15  $\mu\text{m/s}$ . The groove is about 60  $\mu\text{m}$  deep. From [27], reprinted with permission.



Blind via in copper, laser-etched in a sodium nitrate solution; 30 s exposure, 10 W of incident laser power. From [30], reprinted with permission.

**Table 2** Influence of solution concentration on steel and stainless steel for etch of blind vias using 15 W of incident laser power with laser dwell times of 20 s. From [29], reprinted with permission.

Material	Vertical etch depth ( $\mu\text{m}$ )					
	$\text{NaNO}_3$		$\text{K}_2\text{SO}_4$		$\text{NaCl}$	
	5 M	0.5 M	0.5 M	0.1 M	5 M	0.5 M
Steel	60	40	36	14	a	20
Stainless steel	54	40	34	21	a	26

<sup>a</sup>Indicates no measurable etching.

## Conclusion

We have reviewed work on the theory and applications of photothermal-laser-enhanced plating and wet etching that has occurred over the last 20 years. During this period it has been demonstrated that lasers serve as powerful tools for maskless patterning, resulting in high-speed deposition and material removal. Undoubtedly, there exist a multitude of applications not yet fully exploited, particularly in the area of microelectronics. It is clear that laser plating is extremely useful for rapidly generating patterns that could serve as prototypes of new circuit designs. The maskless feature allows for quick turnaround times, allowing for many iterations of the new circuit without the appreciable delays inherent in photolithography. Circuit repair using laser-enhanced electroless or exchange plating is also attractive as applied to very small circuit lines without the need for a mask.

Laser-enhanced jet plating offers means for the rapid application of metal to very localized regions, especially useful in the connector industry, where the method may lead to very large savings in gold. Laser etching offers considerable advantages, particularly for very small parts containing delicate circuitry, such as thin-film heads.

While the laser processes discussed have not yet been put to extensive industrial use, we feel they show great promise for future applications, particularly in the microelectronics industry.

\*\*Trademark or registered trademark of E. I. du Pont de Nemours & Co.

## References

1. R. J. von Gutfeld, E. E. Tynan, R. L. Melcher, and S. E. Blum, "Laser Enhanced Electroplating and Maskless Pattern Generation," *Appl. Phys. Lett.* **35**, 651 (1979).
2. J. Cl. Puijpe, R. E. Acosta, and R. J. von Gutfeld, "Investigation of Laser-Enhanced Electroplating Mechanisms," *J. Electrochem. Soc.* **128**, 2539 (1981).
3. R. J. von Gutfeld, R. E. Acosta, and L. T. Romankiw, "Laser-Enhanced Plating and Etching: Mechanisms and Applications," *IBM J. Res. Develop.* **26**, 136 (1982).
4. R. J. von Gutfeld, "Laser-Enhanced Patterning Using Photothermal Effects: Maskless Plating and Etching," *J. Opt. Soc. Amer. B* **4**, 272 (1987).
5. R. J. von Gutfeld, M. H. Gelchinski, L. T. Romankiw, and D. R. Vigliotti, "Laser-Enhanced Jet Plating: A Method of High-Speed Maskless Patterning," *Appl. Phys. Lett.* **43**, 876 (1983).
6. M. H. Gelchinski, L. T. Romankiw, D. R. Vigliotti, and R. J. von Gutfeld, "Electrochemical and Metallurgical Aspects of Laser-Enhanced Jet Plating of Gold," *J. Electrochem. Soc.* **132**, 2575 (1985).
7. R. J. von Gutfeld and D. R. Vigliotti, "High-Speed Electroplating of Copper Using the Laser-Jet Technique," *Appl. Phys. Lett.* **46**, 1003 (1985).
8. A. Brenner, *Electrodeposition of Alloys: Principles and Practices*, Volumes I and II, Academic Press, Inc., New York, 1963.
9. D. Landolt, "Electrochemical and Materials Science Aspects of Alloy Deposition," *Electrochim. Acta* **39**, 1075 (1994).
10. H. R. Khan, M. Baumgaertner, and Ch. J. Raub, "High Temperature Electrodeposition of Gold-Iron, Gold-Cobalt and Gold-Nickel Layers and their Properties," *Electrodeposition Technology, Theory and Practice*, L. T. Romankiw and D. Turner, Eds., PV 81-17, 1987, The Electrochemical Society, Pennington, NJ, pp. 165-178.
11. H. K. Kuiken, F. E. P. Mikkers, and P. E. Wierenga, "Laser-Enhanced Electroplating on Good Heat-Conducting Bulk Materials," *J. Electrochem. Soc.* **130**, 554 (1983).
12. R. F. Karlceek, V. M. Donnelly, and G. J. Collins, "Laser-Induced Metal Deposition on InP," *J. Appl. Phys.* **53**, 1084 (1982).
13. I. Zouari, F. Lapicque, M. Calvo, and M. Cabrera, "Laser Assisted Metal Electrodeposition: Comprehensive Investigation of Zinc Deposition," *Chem. Eng. Sci.* **45**, 2467 (1990).
14. M. C. Hsiao and C. C. Wan, "The Investigations of Laser-Enhanced Copper Plating on a Good Heat Conducting Copper Foil," *J. Electrochem. Soc.* **138**, 2273 (1991).
15. F. Friedrich and Ch. J. Raub, "Zur Moglichkeit der Laserunterstutzten Electrolyse," *Metall. Oberfläche* **38**, 237 (1984).
16. Yu. V. Seryanov and L. V. Aravina, "Laser-Stimulated Electrodeposition of Sn-Bi Alloy," *Zaschita Metallov.* **28**, 334 (1992) (in Russian).
17. Q. Lin, K. G. Sheppard, M. Datta, and L. T. Romankiw, "Laser-Enhanced Electrodeposition of Lead-Tin Alloys," *J. Electrochem. Soc.* **139**, L62 (1992).
18. L. H. Kulynych, L. T. Romankiw, and R. J. von Gutfeld, "Laser Enhanced Maskless Method for Plating and Simultaneous Plating and Etching of Patterns," U.S. Patent 4,349,583, 1982.
19. M. C. Hsiao and C. C. Wan, "Thermogalvanic Behavior of Acidic Cu<sup>2+</sup>/Cu System Induced by Laser Irradiation," *J. Electrochem. Soc.* **140**, 1334 (1993).
20. L. Mini, C. Giaconia, and C. Arnone, "Copper Patterning on Dielectrics by Laser Writing in Liquid Solution," *Appl. Phys. Lett.* **64**, 3404 (1994).
21. C. J. Chen, "Self Induced Repairing of Conductor Lines," U.S. Patent 4,919,971, 1990.
22. H. Yokoyama, S. Kishida, and K. Washio, "Laser Induced Metal Deposition from Organometallic Solution," *Appl. Phys. Lett.* **44**, 755 (1984).
23. J. H. Chung and K. G. Sheppard, "Laser-Induced, Localized Gold Deposition on Indium Phosphide," *Electrochemical Technology in Electronics*, L. T. Romankiw and T. Osaka, Eds., PV 88-23, 1988, The Electrochemical Society, Pennington, NJ, pp. 351-359.
24. R. J. von Gutfeld, D. R. Vigliotti, O. C. Wells, V. D. Khanna, and E. J. O'Sullivan, "Maskless Laser Patterning of Insulating Films from Salt Solutions," *Appl. Phys. Lett.* **64**, 3348 (1994).
25. R. J. von Gutfeld and D. R. Vigliotti, "High-Speed Electroplating of Copper Using the Laser-Jet Technique," *Appl. Phys. Lett.* **46**, 1003 (1985).
26. S. E. Blum, Z. Kovac, and R. J. von Gutfeld, "Maskless Method for Electroless Plating Patterns," U.S. Patent 4,239,789, 1980.
27. R. J. von Gutfeld and R. T. Hodgson, "Laser Enhanced Etching in KOH," *Appl. Phys. Lett.* **40**, 352 (1982).
28. P. A. Moskowitz, D. R. Vigliotti, and R. J. von Gutfeld, "Laser Micromachining of Polyimide Materials," *Polyimides* **1**, 365 (1984).
29. M. Datta, L. T. Romankiw, D. R. Vigliotti, and R. J. von Gutfeld, "Laser Etching of Metals in Neutral Salt Solutions," *Appl. Phys. Lett.* **51**, 2040 (1987).
30. R. J. von Gutfeld, D. R. Vigliotti, and M. Datta, "Laser Chemical Etching of Metals in Sodium Nitrate Solution," *J. Appl. Phys.* **64**, 5197 (1988).
31. A. Gupta, B. Haba, B. W. Hussey, and L. T. Romankiw, "Laser Etching of Materials in Liquids," U.S. Patent 5,057,184, 1991.
32. B. W. Hussey, B. Haba, and A. Gupta, "Role of Bubbles in Laser-Assisted Wet Etching," *Appl. Phys. Lett.* **58**, 2851 (1991); E. K. Yung, B. W. Hussey, A. Gupta, and L. T. Romankiw, "Laser-Assisted Etching of Manganese-Zinc-Ferrite," *J. Electrochem. Soc.* **136**, 665 (1989).
33. R. Nowak, S. Metev, and G. Sepold, "Laser Chemical Etching of Metals in Liquids," *Mater. & Manuf. Proc.* **9**, 429 (1994).

Received September 1, 1996; accepted for publication September 6, 1997

**Robert J. von Gutfeld** *IBM Research Division, Thomas J. Watson Research Center, P.O. Box 218, Yorktown Heights, New York 10598 (VONG@IBMUS11)*. Dr. von Gutfeld received degrees in physics from Queens College (B.S., 1954), Columbia University (M.A., 1957), and New York University (Ph.D., 1965). After working at Sperry Gyroscope for three years, he joined the IBM Thomas J. Watson Research Center in 1960. He has worked on a variety of subjects, including heat pulses in low-temperature solids, optical memories and optical switching effects in chalcogenides, dye lasers, and the interaction of lasers with solid surfaces. Investigations of laser-enhanced plating and etching followed, and for these Dr. von Gutfeld was awarded the 1984 Research Award of the Electrodeposition Division of the Electrochemical Society. Most recently his work has centered on developing magnetic tags for identification and antitheft applications. Dr. von Gutfeld is a member of the Electrochemical Society and the Optical Society of America, and a Fellow of the American Physical Society.

**Keith G. Sheppard** *Stevens Institute of Technology, Hoboken, New Jersey 07030 (ksheppar@stevens-tech.edu)*. Dr. Sheppard received the Bachelor of Science degree in metallurgy from Leeds University in 1971 and the Ph.D. from the University of Birmingham in England in 1980. His thesis research was on the structure and properties of pure gold and silver electrodeposits for electronic devices. Prior to his graduate work, he spent four years in industry, first as a market research executive and then in metal powder synthesis. In 1979 Dr. Sheppard joined the Stevens Institute of Technology, where he is a Professor of Materials Science and Engineering and Associate Dean of Engineering. His research interests are in research and development of electrochemical surface modification and corrosion. Dr. Sheppard is a past Chairman of the Electrodeposition Division of the Electrochemical Society, for which he has co-organized six international symposia on electrodeposition topics. Other professional affiliations include the American Electroplaters and Surface Finishers Society, NACE International, and the American Society for Engineering Education.